Supporting Information

Unveiling thermolysis pathways of ZIF-8 and ZIF-67 by employing *in situ* structural characterizations

Chunhui Wu,[b] Donggang Xie,[b] Yingjie Mei,[a] Zhifeng Xiu,[b] Kristin M. Poduska,[c] Dacheng Li,[d] Ben Xu,[a, b*] and Daofeng Sun [a, b]

a. College of Material Science and Engineering, China University of Petroleum (East China), Qingdao, Shandong, 266580, People's Republic of China.

b. College of Science, China University of Petroleum (East China), Qingdao, Shandong, 266580, People's Republic of China.

c. Department of Physics and Physical Oceanography, Memorial University of Newfoundland, St. John's, NL, A1B3X7, Canada.

d. Shandong Provincial Key Laboratory of Chemical Energy Storage and Novel Cell Technology, School of Chemistry and Chemical Engineering, Liaocheng University, Liaocheng, 252059, People's Republic of China

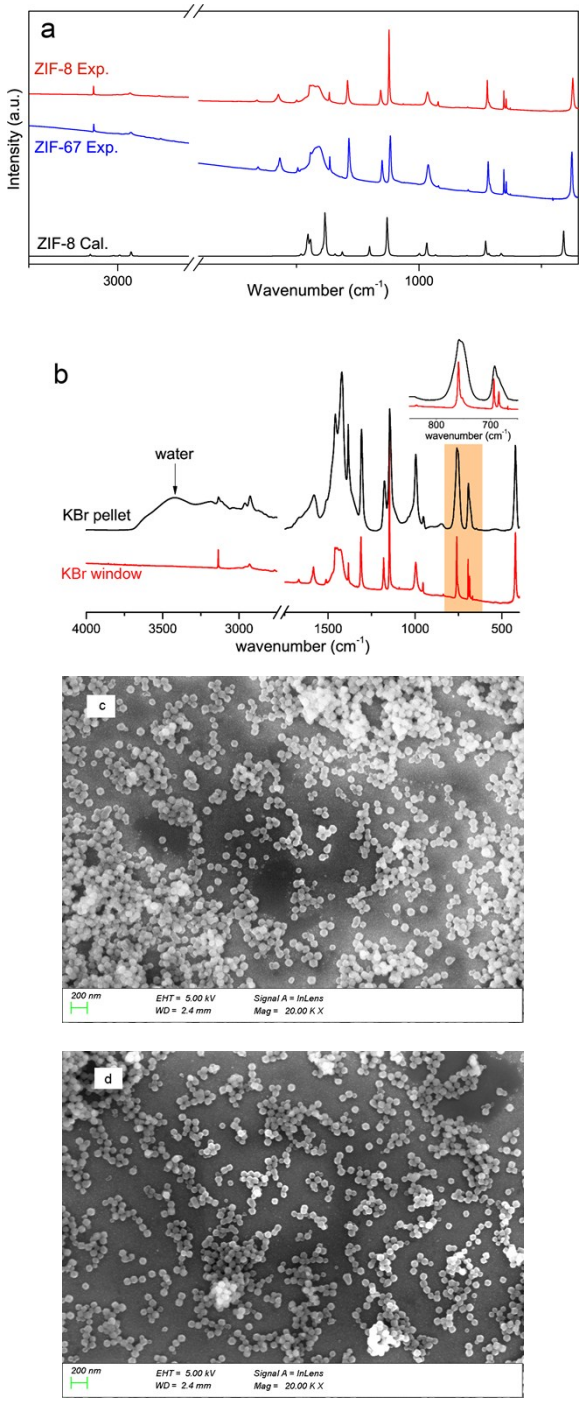

Fig. S1 The *ex situ* FTIR spectra of ZIF-8 and ZIF-67 (a), and comparison between the FTIR spectra of ZIF-8 collected using KBr pellets and KBr windows. The inset shows the zoomed-in peaks from 850 to 650 cm^{-1}. The spectrum collected using the KBr window (b) displays much sharper and narrower peaks. The narrower peaks are due to the smaller and more uniform ZIF-8 particle sizes during the KBr window measurement. Representative SEM images of "drop-coated" ZIF-8 and ZIF-67 samples are shown in (c) and (d).

Table S1. Peak positions and vibrational mode assignments for ZIF-8 (experiment and calculated) and ZIF-67 (experiment).

Band assignment[a]	ZIF-8 Exp. (cm^{-1})	ZIF-67 Exp. (cm^{-1})	ZIF-8 Cal. (cm^{-1})[b]
Methyl in-plane bend (S)	422	425	410 (-12)
Ring out-of-plane bend (M)	685	685	665 (-20)
Methyl stretch (S)	694	694	683 (-11)
H_{ring} symmetric out-of-plane bend (S)	759	756	728 (-31)
H_{ring} asymmetric out-of-plane bend (VW)	837	8359	804 (-33)
Ring in-plane bend (W/VW)	953	952	932 (-21)
H_{methyl} bend (S)	995	992	971 (-24)
H_{ring} scissor + H_{methyl} bend (VW)	1091	-	998 (-93)
H_{ring} wag (VS/S)	1147	1142	1130 (-17)
Ring breathing (C-N symmetric stretch) (S)	1180	1175	1201 (21)
H_{methyl} scissor(M)	1311	1304	1312 (1)
Ring deformation (C-N asymmetric stretch) (S)	1380	1381	1342 (-38)
H_{methyl} bend (S)	1400~1500	1400~1500	1380~1420
C=C stretch+C_{ring}-C_{methyl} stretch (W)	1512	1507	1442 (-70)
Ring breathing (C=C stretch) (M)	1584	1578	1452 (-132)
H_{methyl} symmetric stretch (W)	2932	2927	2926 (-6)
H_{methyl} asymmetric stretch (VW)	2957	2954	2989 (35)
H_{ring} symmetric stretch (M)	3136	3135	3154 (18)

[a] S, M, W, and VW indicate strong, medium, weak, and very weak peak intensities, respectively.

[b] The values in parentheses indicate differences between experimental and calculated results.

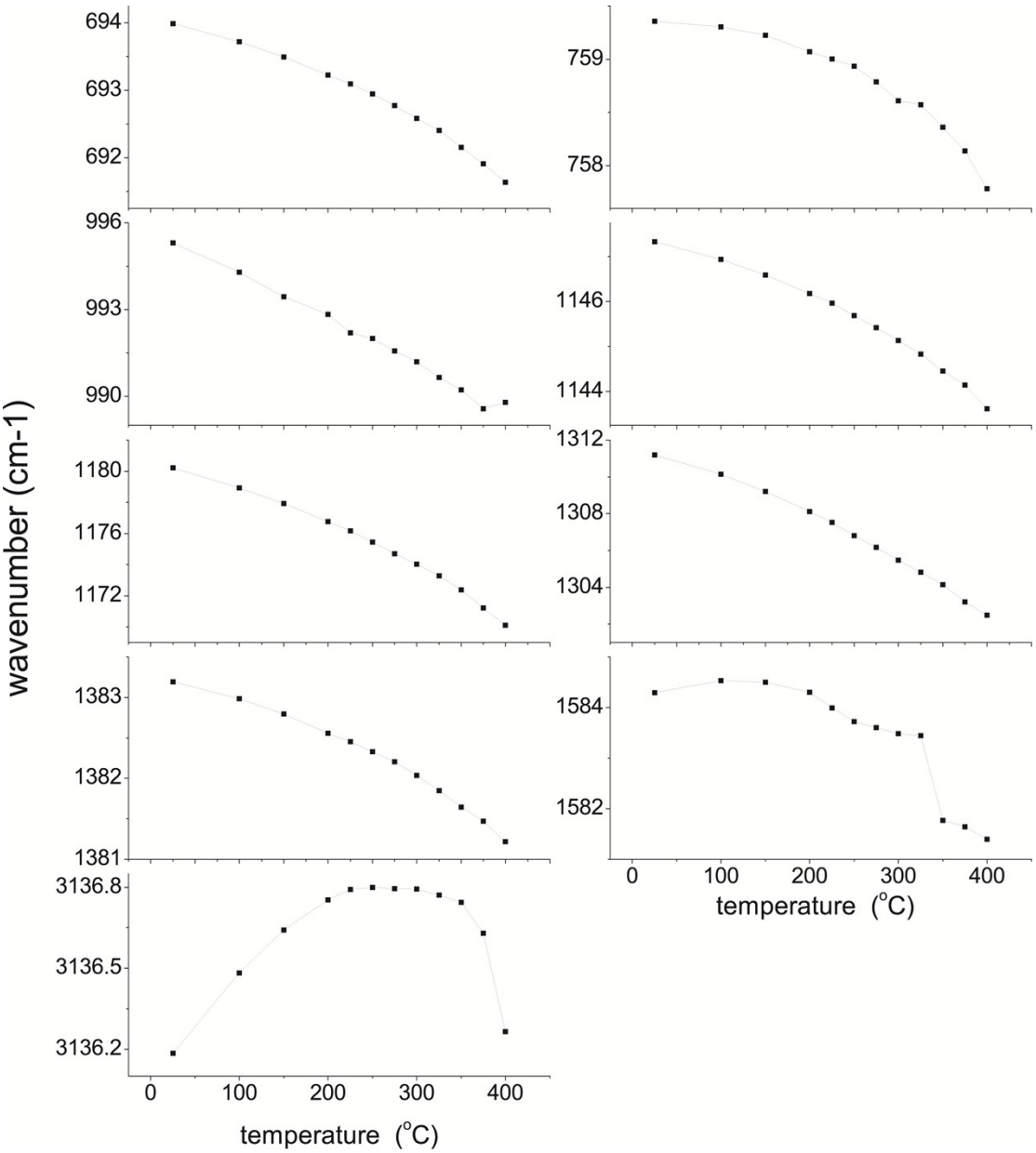

Figure S2 The peak position changes in temperature-dependent IR spectra of ZIF-8.

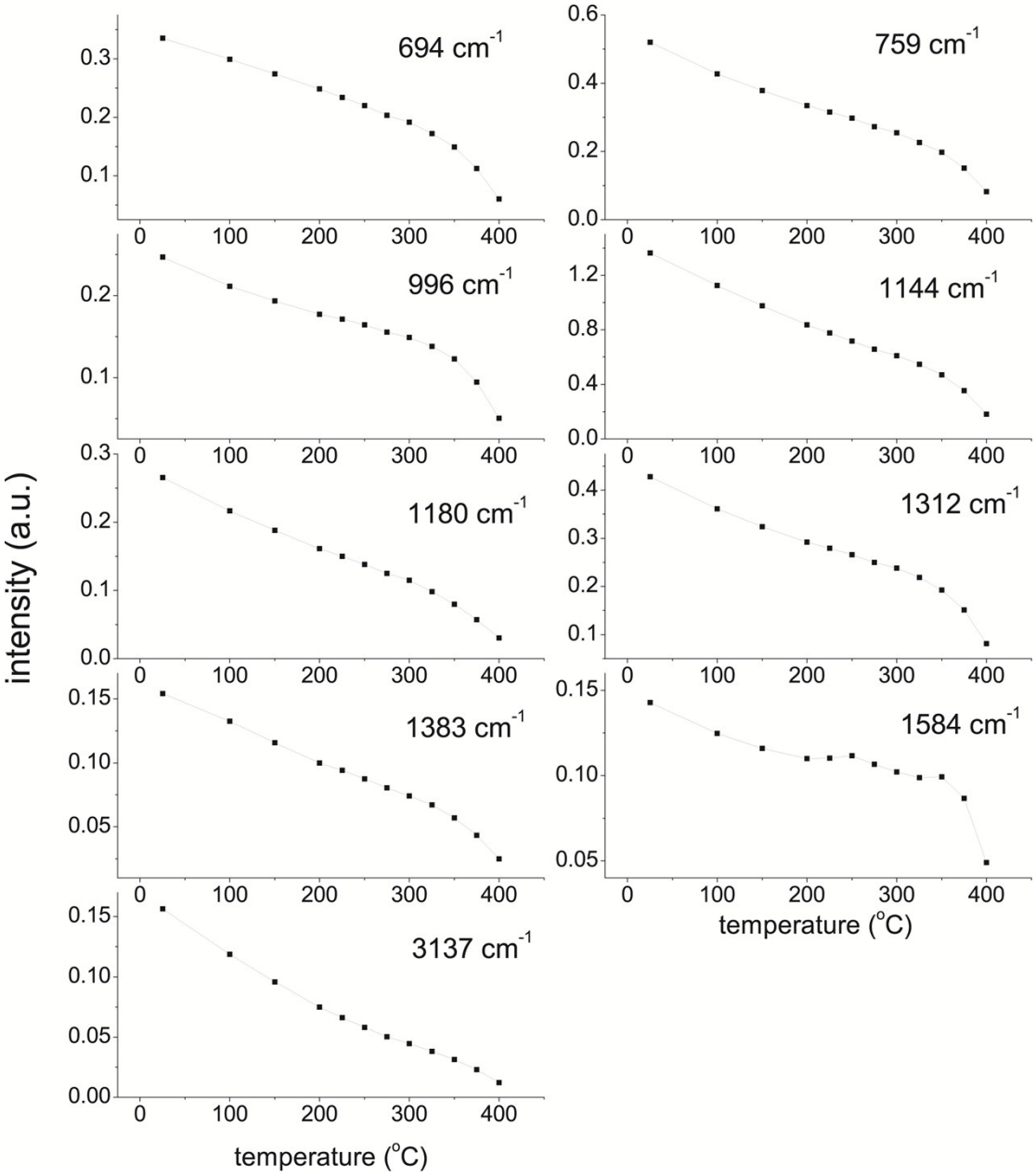

Figure S3 The peak intensity changes in temperature-dependent IR spectra of ZIF-8.

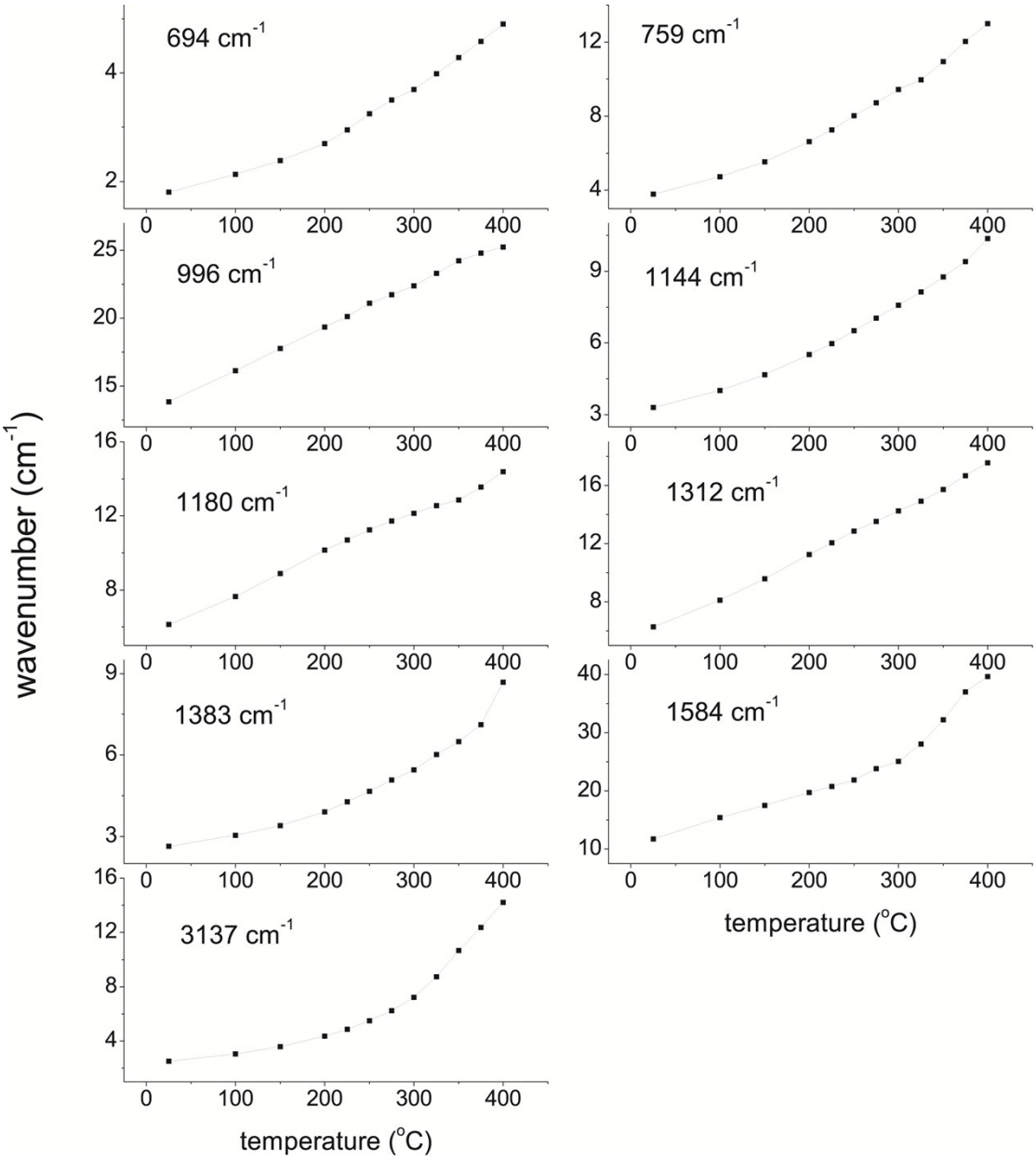

Figure S4 The peak width changes in temperature-dependent IR spectra of ZIF-8.

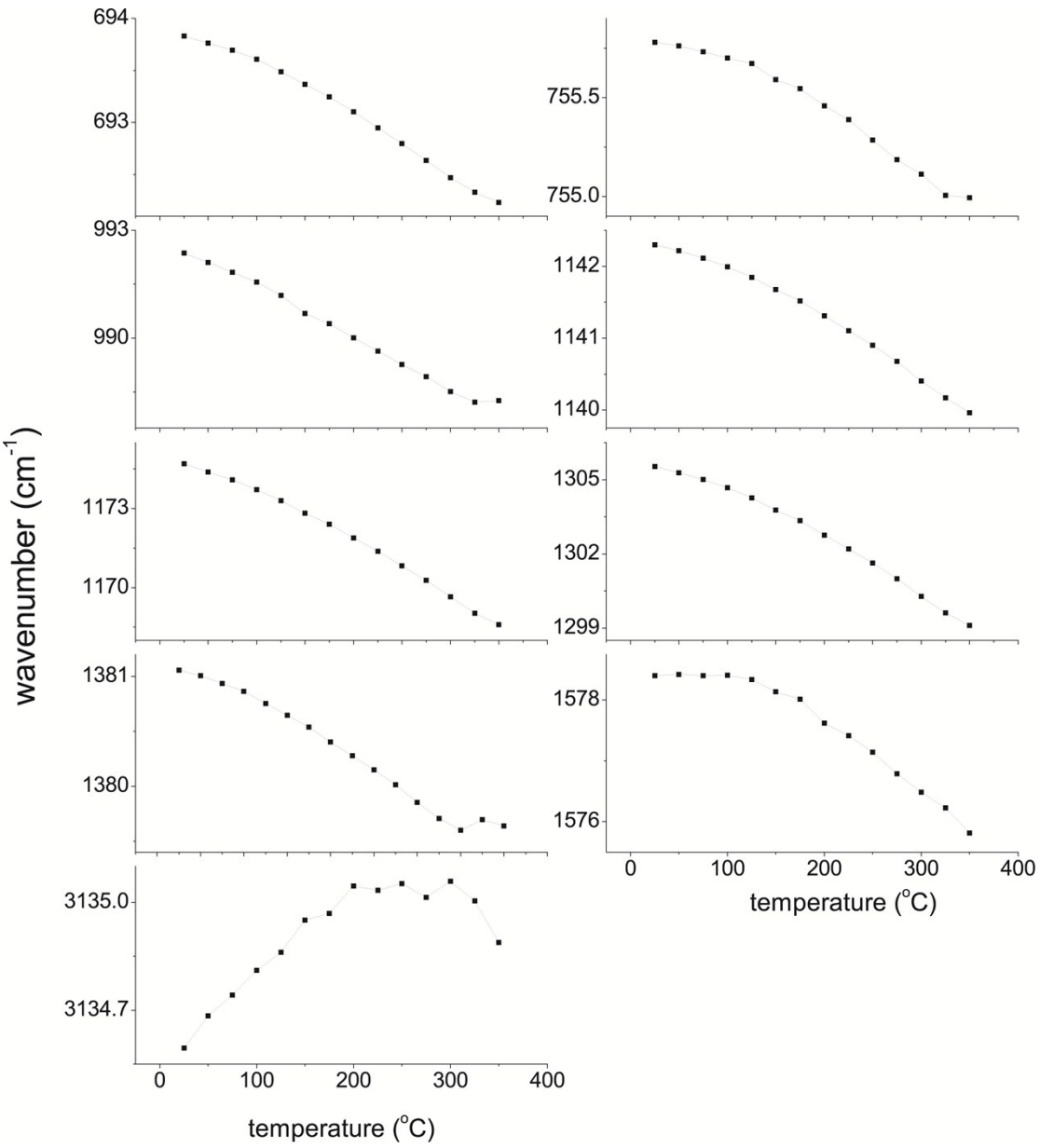

Figure S5 The peak position changes in temperature-dependent IR spectra of ZIF-67.

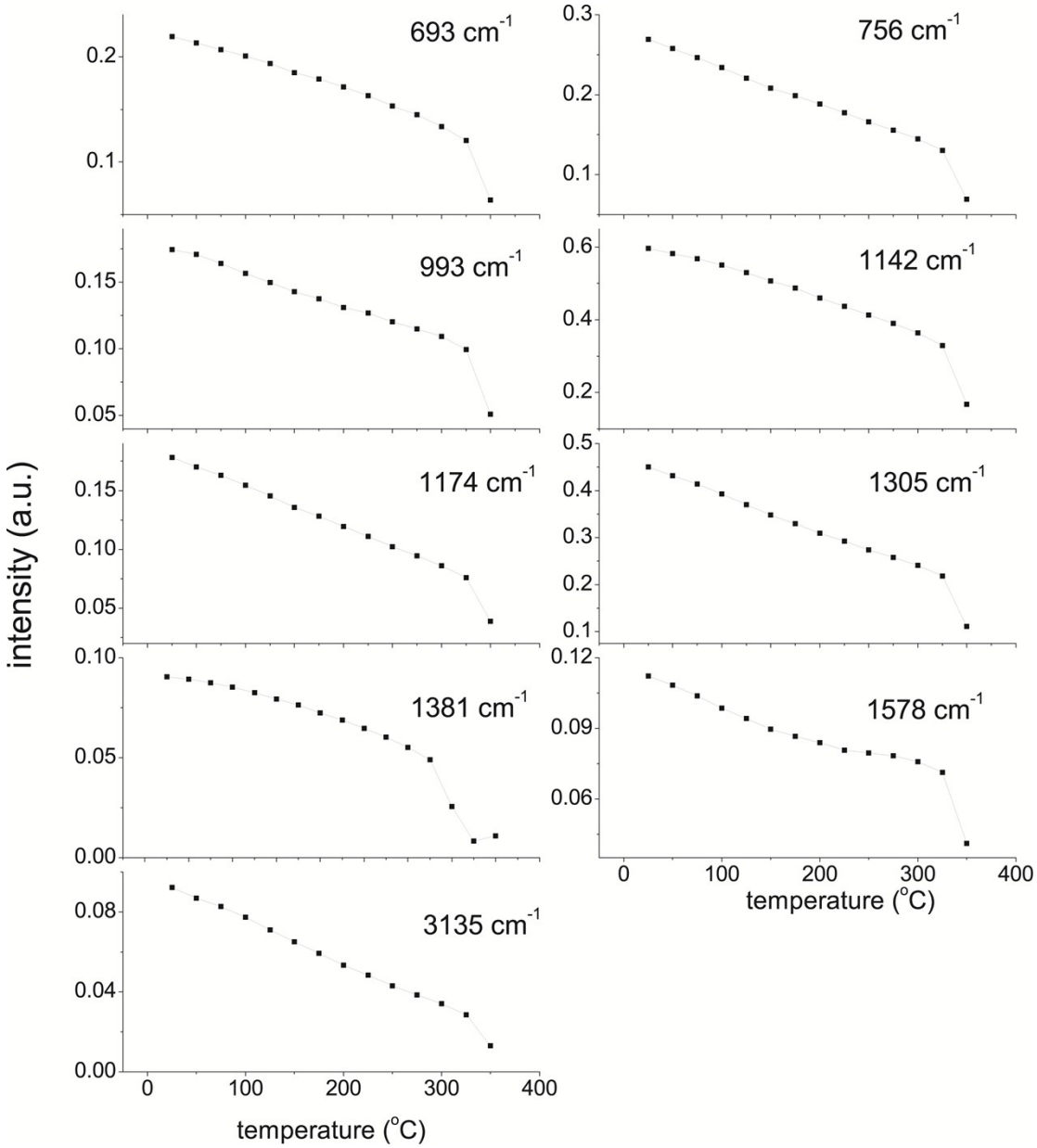

Figure S6 The peak intensity changes in temperature-dependent IR spectra of ZIF-67.

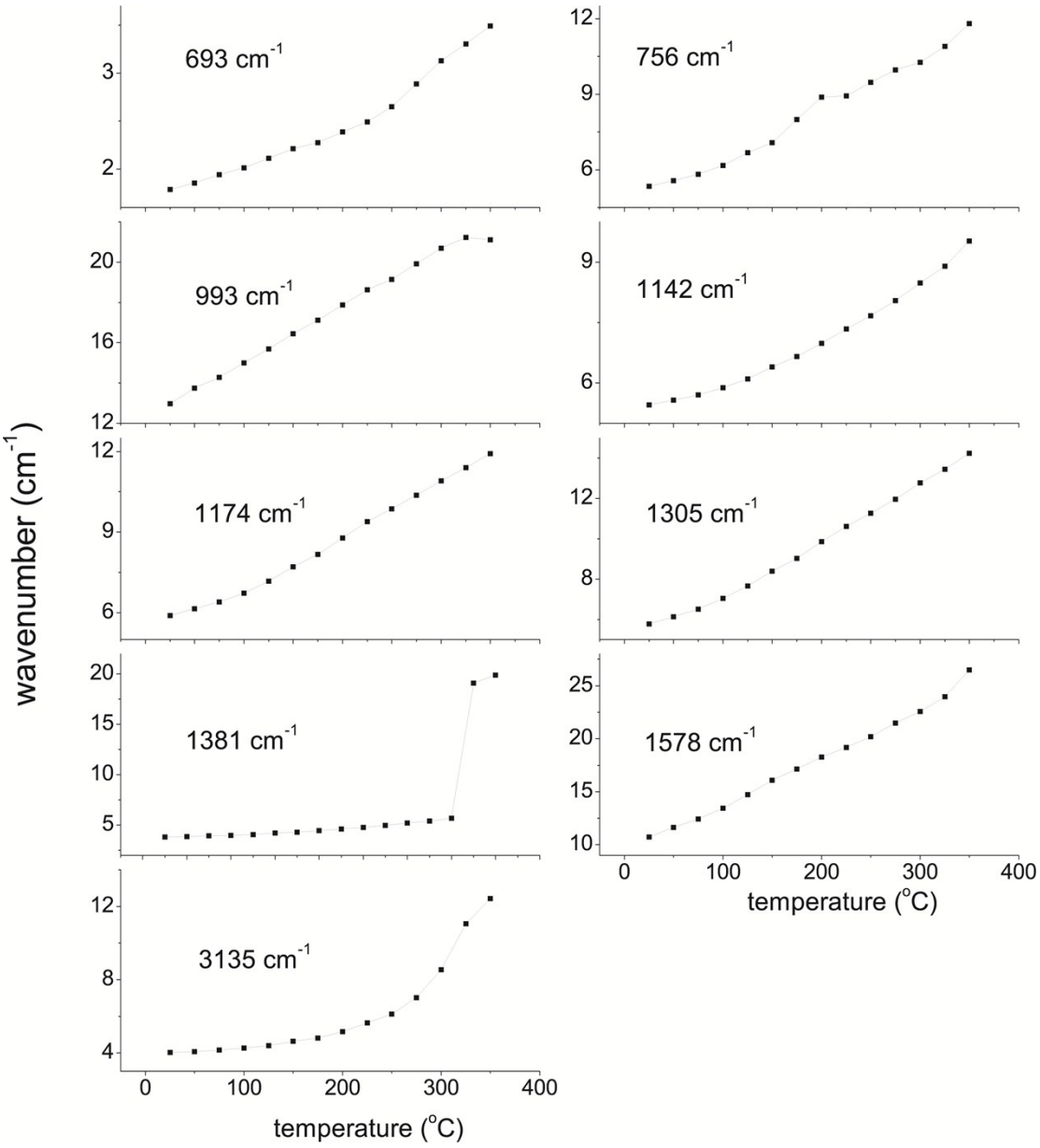

Figure S7 The peak width changes in temperature-dependent IR spectra of ZIF-67.

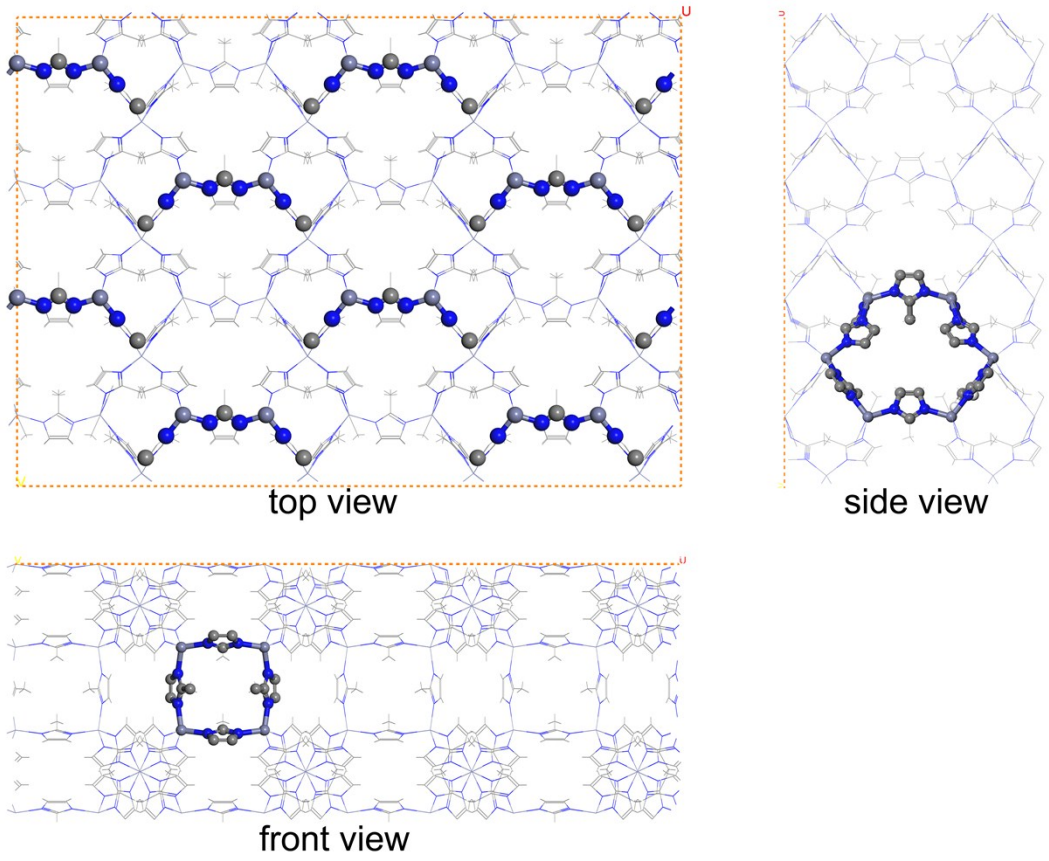

Fig. S8 The (011) plane of ZIF-8. The Co-N bonds are on this plane. The inter-planar distances are associated with the ZIF-8 frame. Hydrogen atoms are hidden for clarity.

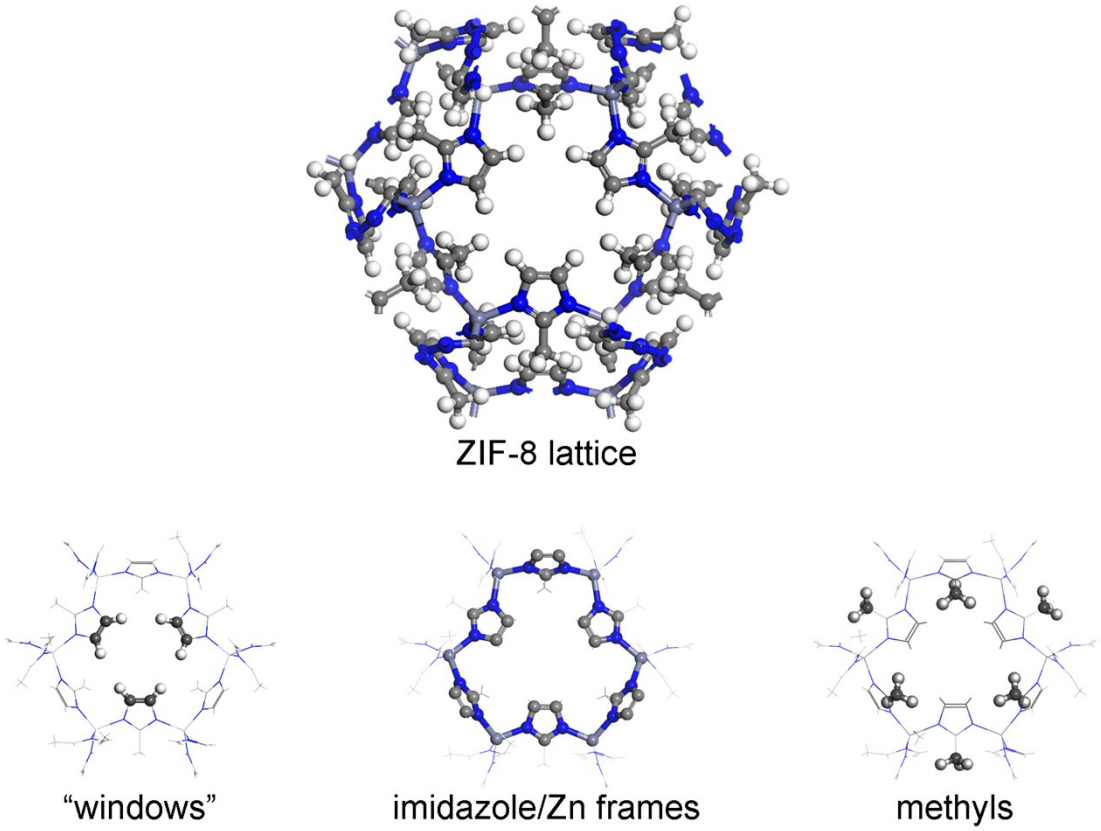

Figure S9 The lattice of ZIF-8/67. The lattice is composed of “window” fractions, “imidazole-metal” fractions, and “methyl” fractions. Zinc, nitrogen, carbon, and hydrogen atoms are purple, blue, grey, and white, respectively.

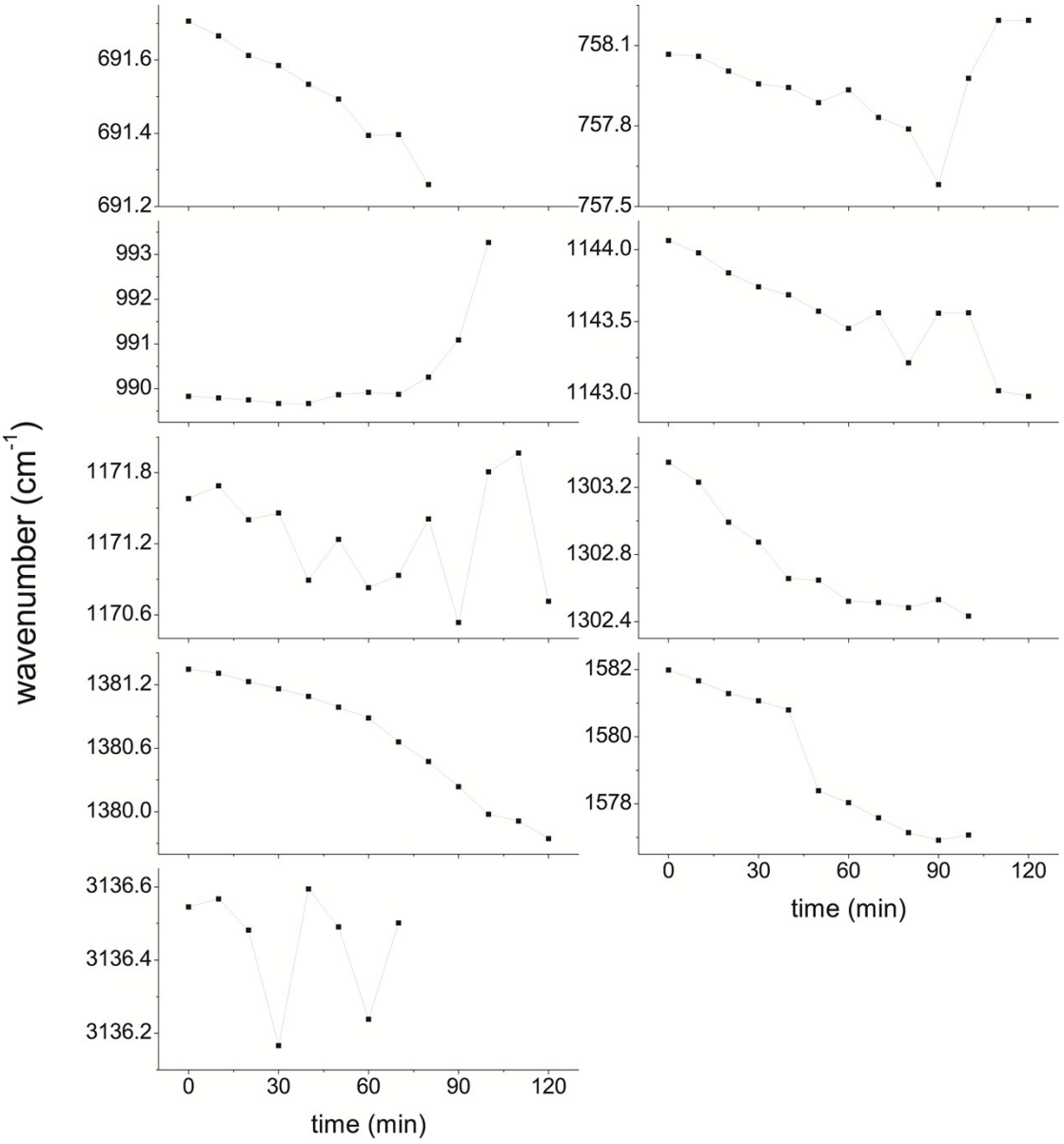

Figure S10 The peak position changes in time-dependent IR spectra of ZIF-8.

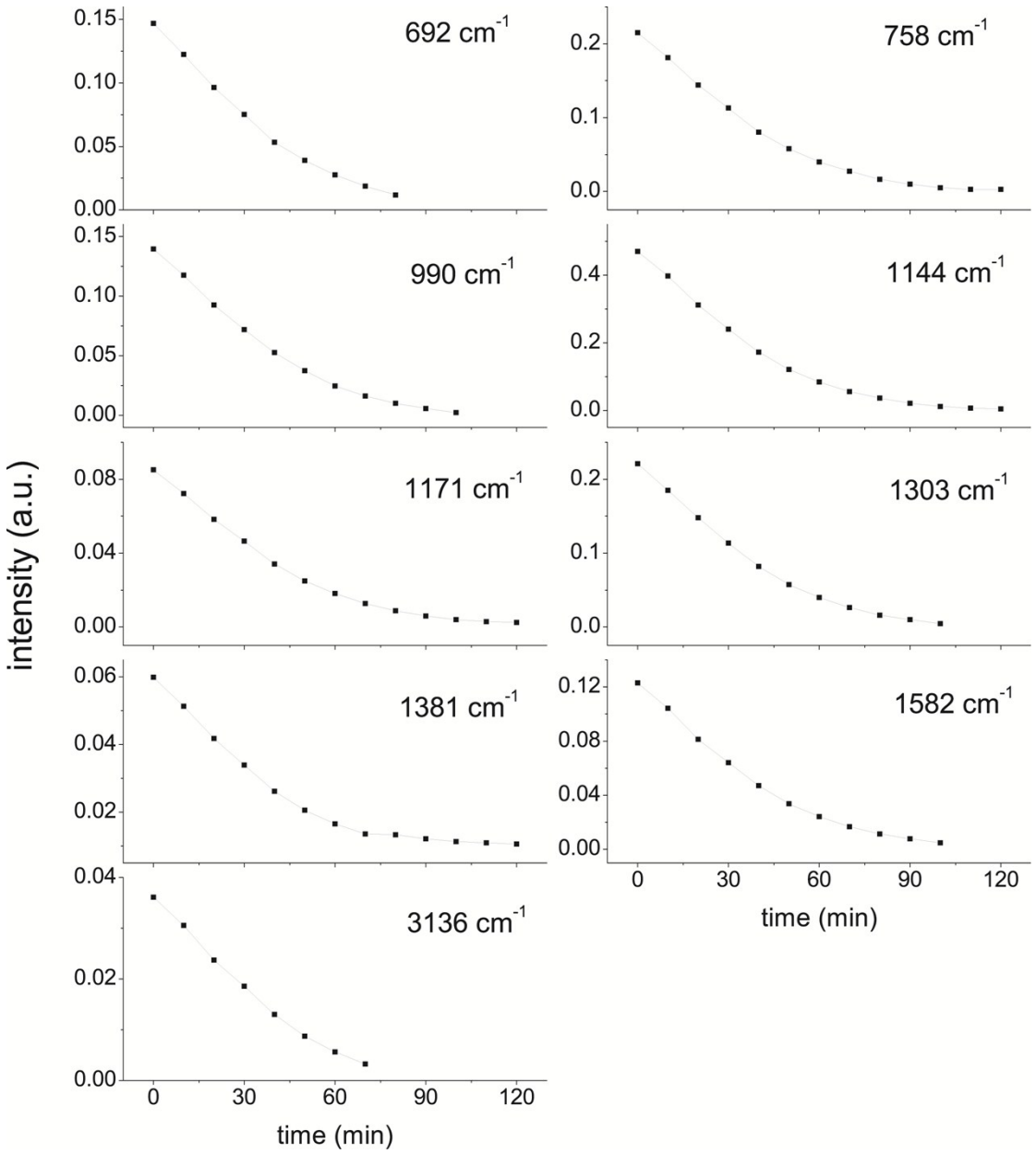

Figure S11 The peak intensity changes in time-dependent IR spectra of ZIF-8.

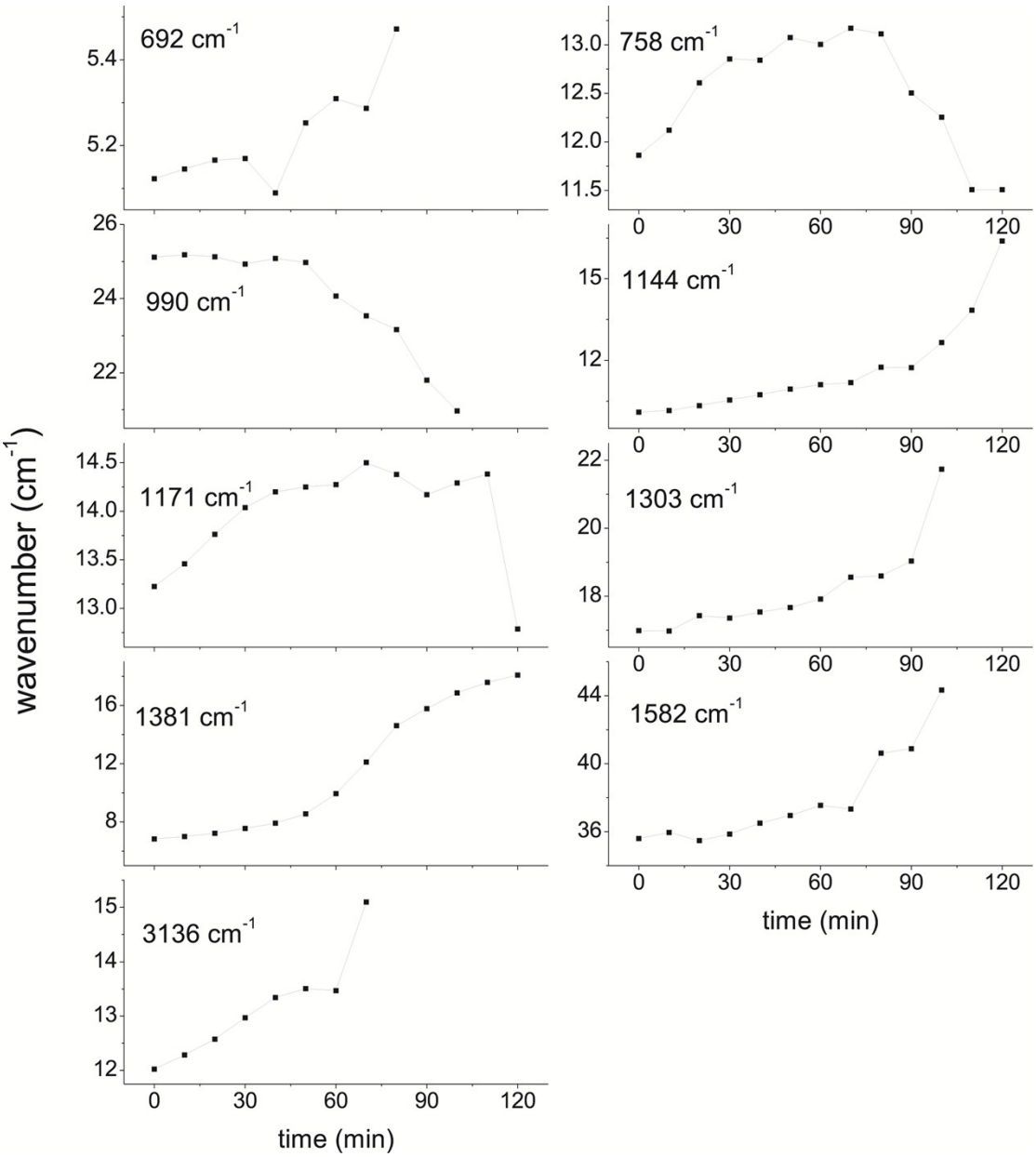

Figure S12 The peak width changes in time-dependent IR spectra of ZIF-8.

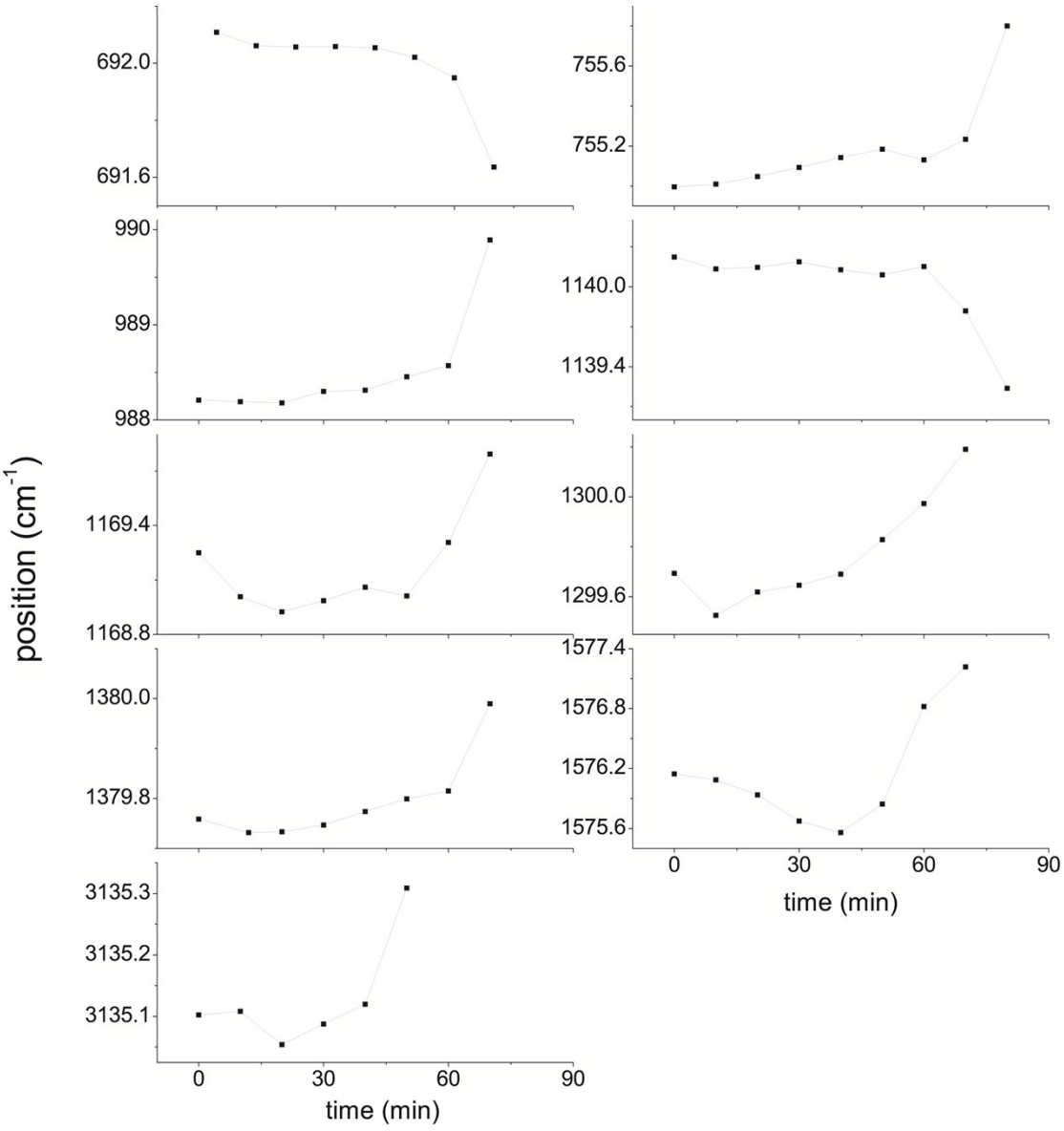

Figure S13 The peak position changes in time-dependent IR spectra of ZIF-67.

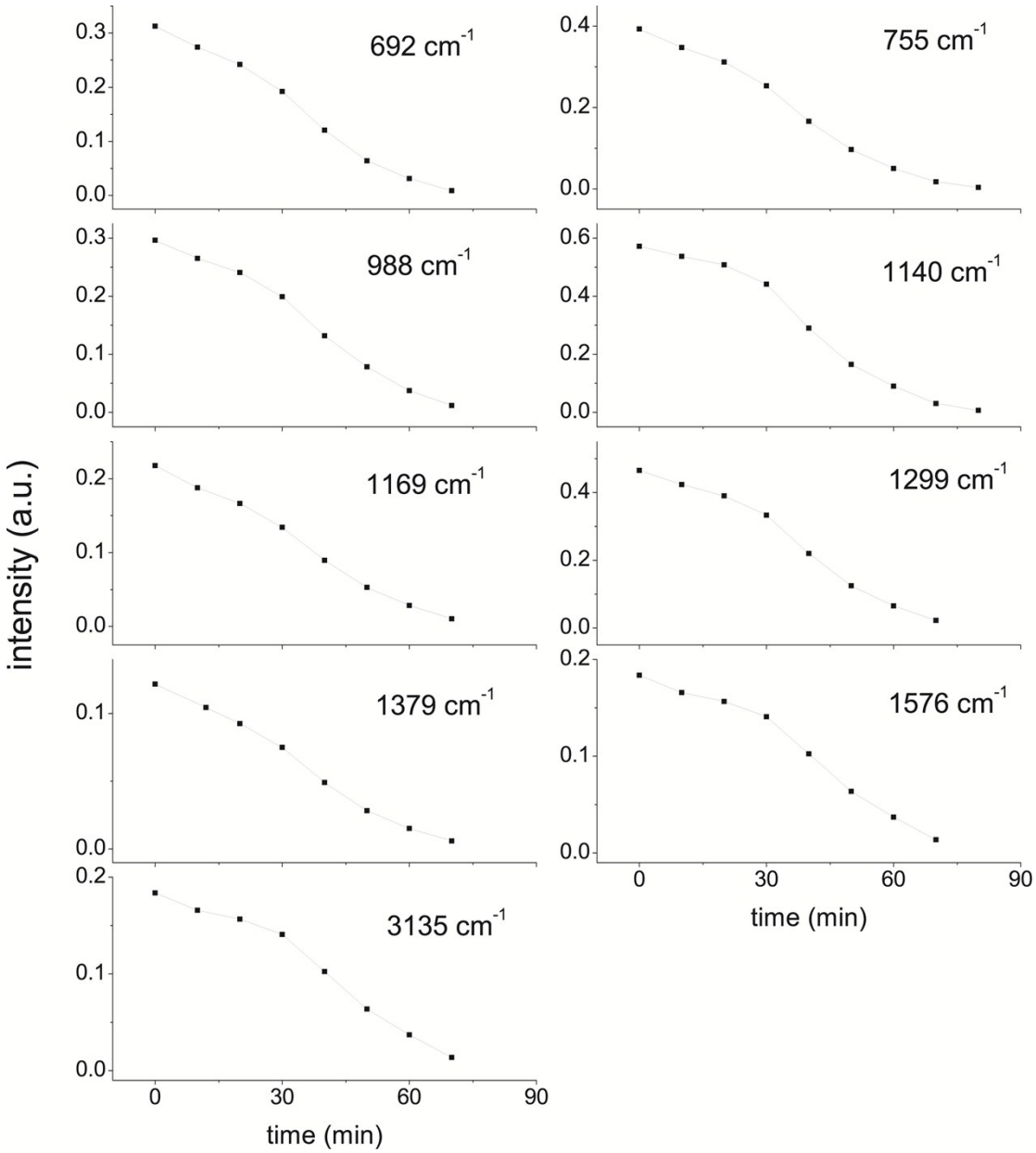

Figure S14 The peak intensity changes in time-dependent IR spectra of ZIF-67.

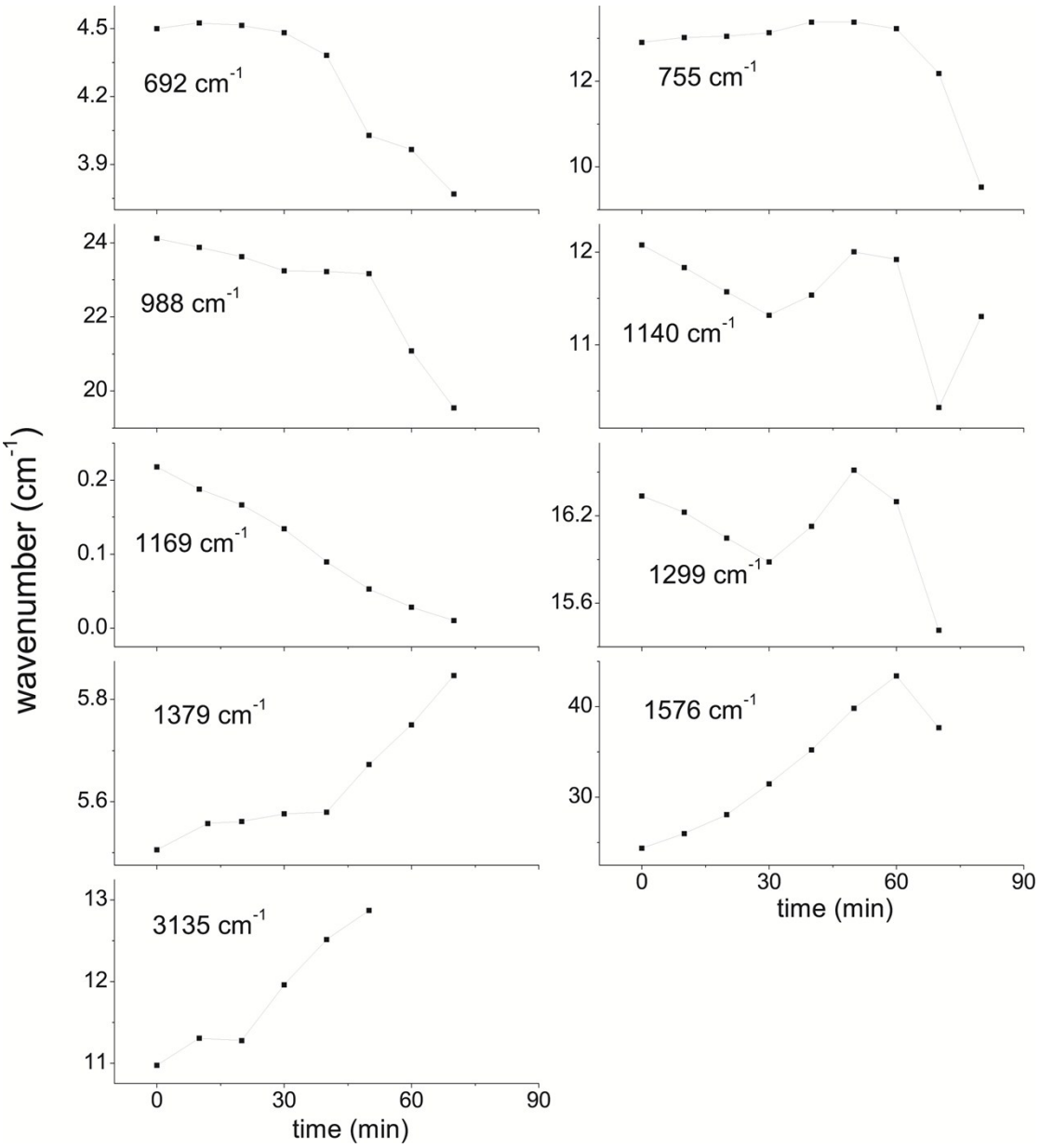

Figure S15 The peak width changes in time-dependent IR spectra of ZIF-67.

Table S2 The fitted results of H_{ring} wagging intensity vs time plots to Avrami's model for both ZIF-8 and ZIF-67

	ZIF-8	ZIF-67
k	0.0252±0.0001	0.0213±0.0003
n	1.33±0.01	2.7±0.1

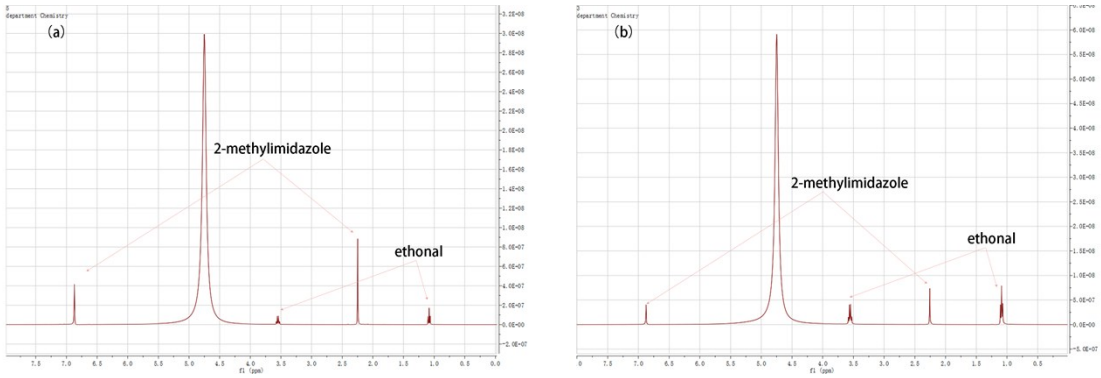

Figure S16 Solution NMR spectra of heated ZIF-8 (a) and ZIF-67 (b). ZIF-8 was heated at 350 ℃ for 20 minutes and ZIF-67 was heated at 300 ℃ for 10 minutes. The heated samples were immersed in Na_2S deuterium oxide solution to obtain the solution for NMR measurements. It is clear that there are only 2-methylimidazole peaks and ethonal peaks (the samples were rinsed with ethonal). No other organic peaks were observed.